

## Palladium-Mediated Synthesis of a Near-Infrared Fluorescent K<sup>+</sup> Sensor

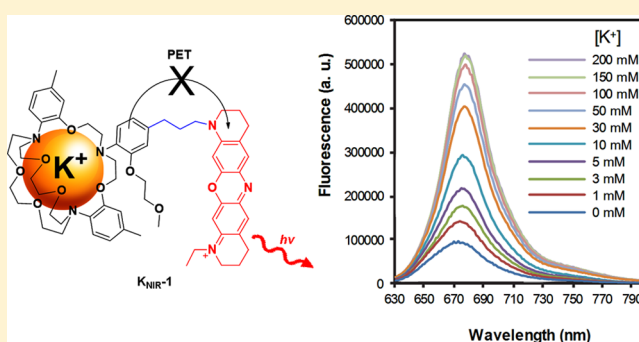
H. M. Dhammika Bandara,<sup>†</sup> Zhengmao Hua,<sup>†</sup> Mei Zhang,<sup>†</sup> Steven M. Pauff,<sup>†,§</sup> Stephen C. Miller,<sup>†,||</sup> Elizabeth A. Colby Davie,<sup>‡</sup> and William R. Kobertz<sup>\*,†,||</sup>

<sup>†</sup>Department of Biochemistry and Molecular Pharmacology, Programs in Neuroscience and Chemical Biology, University of Massachusetts Medical School, 364 Plantation Street, Worcester, Massachusetts 01605, United States

<sup>‡</sup>Department of Natural Sciences, Assumption College, 500 Salisbury Street, Worcester, Massachusetts 01609, United States

### S Supporting Information

**ABSTRACT:** Potassium (K<sup>+</sup>) exits electrically excitable cells during normal and pathophysiological activity. Currently, K<sup>+</sup>-sensitive electrodes and electrical measurements are the primary tools to detect K<sup>+</sup> fluxes. Here, we describe the synthesis of a near-IR, oxazine fluorescent K<sup>+</sup> sensor (K<sub>NIR-1</sub>) with a dissociation constant suited for detecting changes in intracellular and extracellular K<sup>+</sup> concentrations. K<sub>NIR-1</sub> treatment of cells expressing voltage-gated K<sup>+</sup> channels enabled the visualization of intracellular K<sup>+</sup> depletion upon channel opening and restoration of cytoplasmic K<sup>+</sup> after channel closing.



Neuronal and muscle excitability, cardiac rhythmicity, vasodilation, insulin secretion, and renal function all require the spatiotemporal release of potassium (K<sup>+</sup>) ions from cells and tissues.<sup>1–6</sup> During normal physical activity, the concentration of extracellular K<sup>+</sup> surrounding human muscle nearly triples, rising from 3.5 to 10 mM.<sup>2,3</sup> This substantial change in extracellular K<sup>+</sup> is predicted to be even greater in the transverse tubules,<sup>7–9</sup> though current methods do not allow for accurate measurements in these microscopic invaginations. Regulated K<sup>+</sup> efflux is also essential for the developing pancreas, kidney, and vestibular and cochlear endolymphs.<sup>5,6,10</sup> Accordingly, dysregulated exit of cellular K<sup>+</sup> from tissues has been associated with a multitude disease states from epilepsy,<sup>11</sup> migraine auras,<sup>12</sup> hypokalemic periodic paralysis,<sup>13</sup> and cardiac arrhythmias<sup>14</sup> to neonatal diabetes,<sup>15</sup> hyperkalemia,<sup>16</sup> and congenital deafness.<sup>17</sup> Electrical measurements and potassium-sensitive electrodes provide pinpoint accuracy of K<sup>+</sup> efflux, but both approaches are invasive, technically demanding, and time-consuming compared to the small molecule<sup>18</sup> and genetically encodable fluorescent-based sensors<sup>19,20</sup> that have revolutionized the intracellular signaling field. Although several small molecule fluorescent K<sup>+</sup> sensors have been synthesized,<sup>21–25</sup> the current cadre of water-soluble, visible-light K<sup>+</sup> sensors is not routinely used to visualize K<sup>+</sup> fluxes from cells, tissues, or animal models. Part of the problem is that cells and tissues absorb visible light,<sup>26</sup> resulting in cellular damage, loss of signal, and unwanted autofluorescence. However, the major stumbling block has been the inefficient and limited routes to attach fluorophores to the K<sup>+</sup> binding domain,<sup>23–25</sup> which has hampered the application of these sensors for detecting K<sup>+</sup> accumulation and depletion.

To overcome these barriers, we sought a synthesis of a near-IR fluorescent K<sup>+</sup> sensor where fluorophore attachment to the K<sup>+</sup> binding domain was facile. For the potassium-selective binding domain, we chose a triazacryptand (TAC) to detect physiological and pathophysiological K<sup>+</sup> concentrations for three reasons (Figure 1): (1) The TAC ion binding site is

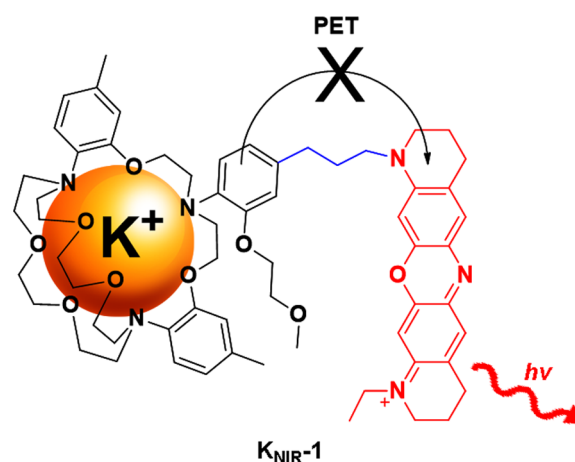


**Figure 1.** Near-IR K<sup>+</sup> sensor K<sub>NIR-1</sub> consists of a TAC K<sup>+</sup> binding domain covalently linked to an oxazine fluorophore. Binding of K<sup>+</sup> to the TAC domain quenches PET from the o-alkoxyaniline moiety to the oxazine fluorophore, resulting in enhanced fluorescence emission.

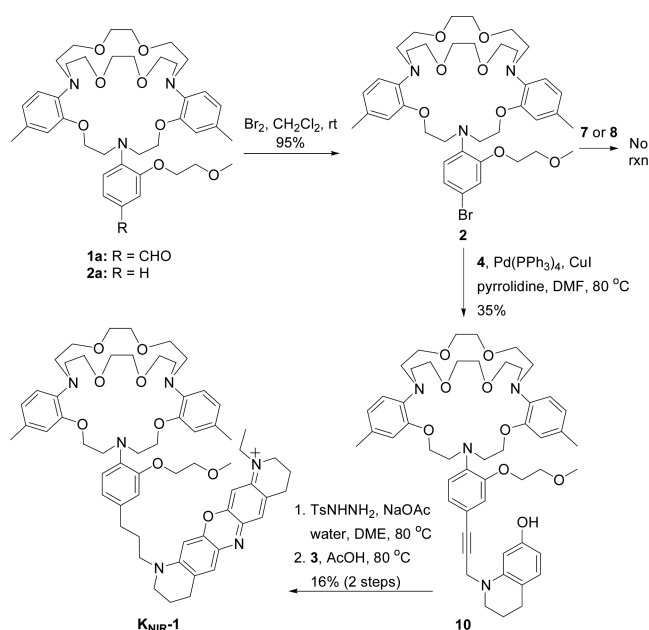
Received: April 10, 2017

Published: June 30, 2017

slightly larger than the  $K^+$  ion diameter, yielding an apparent millimolar  $K_d$  for potassium.<sup>23–25</sup> (2) TAC does not measurably bind to the smaller and physiologically abundant extracellular cations:<sup>23–25</sup>  $Na^+$ ,  $Ca^{2+}$ , and  $Mg^{2+}$ . (3) The electron-rich aromatic groups of TAC enable  $K^+$  sensing via photoinduced electron transfer (PET) with fluorophores. Given this flexibility, we opted to synthesize a  $K^+$  sensor with an oxazine dye  $K_{NIR-1}$  (Figure 1) because of its compact structure, photostability,<sup>27</sup> amenability to PET quenching,<sup>28</sup> and excitation and fluorescence emission wavelengths in the near-IR region (650–900 nm).<sup>29</sup>

Previous syntheses of visible-light  $K^+$  sensors have directly coupled the fluorophore to the TAC binding domain using aldehyde precursor 1a (TAC–CHO, Scheme 1). Similar to the

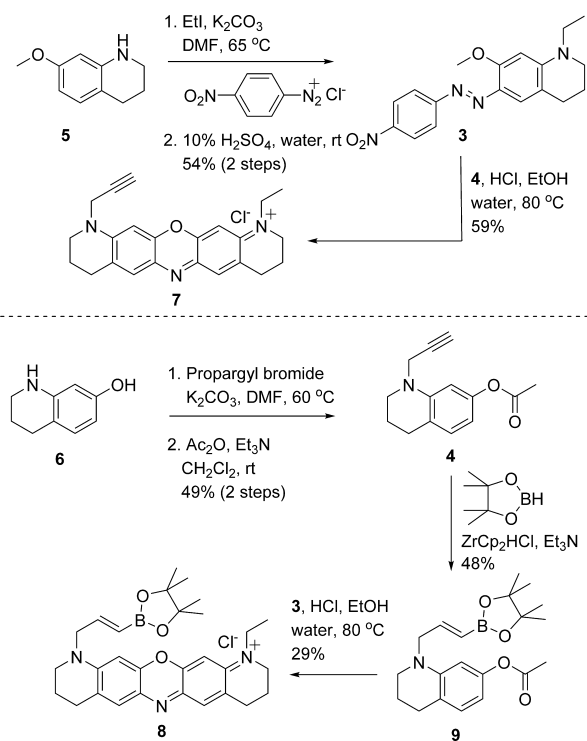
**Scheme 1. Synthesis of Near-IR Fluorescent  $K^+$  Sensor  $K_{NIR-1}$**



reported low yields in the literature,<sup>23–25</sup> our attempts to form a near-IR dye utilizing TAC–CHO were unsuccessful. Stymied by the inability to efficiently derivatize TAC–CHO, we pursued a palladium-mediated aryl coupling approach to append fluorophores to the TAC  $K^+$  binding domain. Aryl halogenation of the TAC binding domain (Scheme 1) is ideal for selective modification of the *o*-alkoxyaniline PET donor because it is the only aromatic ring that is not blocked by a methyl group in the *para* position. Treatment of 1b with bromine resulted in the selective and near quantitative bromination of the aryl PET donor ring. Iodination of TAC also proceeds quantitatively; however, the iodinated product is more challenging to purify and thus was not pursued further.

With halogenated TAC 2 in hand, we initially envisioned attaching an intact oxazine fluorophore via palladium-catalyzed cross-coupling reactions (e.g., Sonogashira, Suzuki, Stille, etc.). To synthesize the oxazine dye with a pendant prop-2-yn-1-yl group, aryl azobenzene 3 and prop-2-yn-1-yl tetrahydroquinoline 4 were prepared separately and then reacted together in acid (Scheme 2). To prepare the aryl azobenzene 3, 7-methoxytetrahydroquinoline 5 was first *N*-alkylated with iodoethane and then subsequently reacted with 4-nitrodiazobenzene. The tetrahydroquinoline 4 was synthesized by

**Scheme 2. Synthesis of Oxazine Dyes and Precursors for Palladium-Based Coupling Reactions**



*N*-alkylation of 7-hydroxytetrahydroquinoline 6 with 3-bromo-1-propyne, followed by acetylation of the 7-hydroxy group with acetic anhydride. Condensation of aryl azobenzene 3 and prop-2-yn-1-yl tetrahydroquinoline 4 in acetic acid or 1.5% hydrochloric acid yielded the desired oxazine dye 7. Synthesis of the borylated oxazine 8 was accomplished by borylation of tetrahydroquinoline 4 with pinacol borane to generate boronate ester 9, followed by condensation between 9 and arylazobenzene 3 in 1.5% hydrochloric acid.

Despite trying several different palladium ligands, cocatalysts, counteranions, and solvents, the Sonogashira reaction between 2 and prop-2-yn-1-yl oxazine dye 7 did not occur (Scheme 1). Suzuki couplings between 2 and boronate ester oxazine dye 8 were also unsuccessful. To test whether the lack of reactivity was due to the seemingly cantankerous TAC ligand or the oxazine dye, we repeated the palladium-based reactions with the oxazine dye precursors 4 and 9 shown in Scheme 2. Surprisingly, the Sonogashira reaction between 2 and 4 proceeded smoothly, yielding TAC-alkyne 10 (Scheme 1), lacking the acetate group, which falls off during the palladium-mediated coupling. TAC-Br 2 was also amenable to a Suzuki coupling with boronate ester 9 shown in Scheme 2 (data not shown), suggesting that the positive-charge and/or reduction of the intact dye may impede palladium-catalyzed aryl coupling reactions. Palladium impurities in the resultant alkyne were removed using a palladium scavenger (SiliaMetS DMT), and the purified alkyne was reduced by tosyl hydrazide hydrogenation. Failure to remove all of the palladium impurities results in cleavage of the tetrahydroquinoline from the TAC  $K^+$  binding domain during reduction. Oxazine dye formation between reduced 10 and aryl azobenzene 3 proceeded in acetic acid as previously reported<sup>30</sup> and was purified by reverse phase HPLC. Interestingly, dye formation to afford TAC-oxazine  $K_{NIR-1}$  did not proceed in 1.5% hydrochloric, trifluoroacetic, or

formic acid, suggesting that protonation of the TAC K<sup>+</sup> binding domain hinders oxazine dye formation.

The fluorescence of TAC-oxazine K<sub>NIR-1</sub> was initially tested in the presence of various concentrations of physiological extracellular cations: Na<sup>+</sup>, Ca<sup>2+</sup>, Mg<sup>2+</sup>, and K<sup>+</sup>. Figure 2A shows

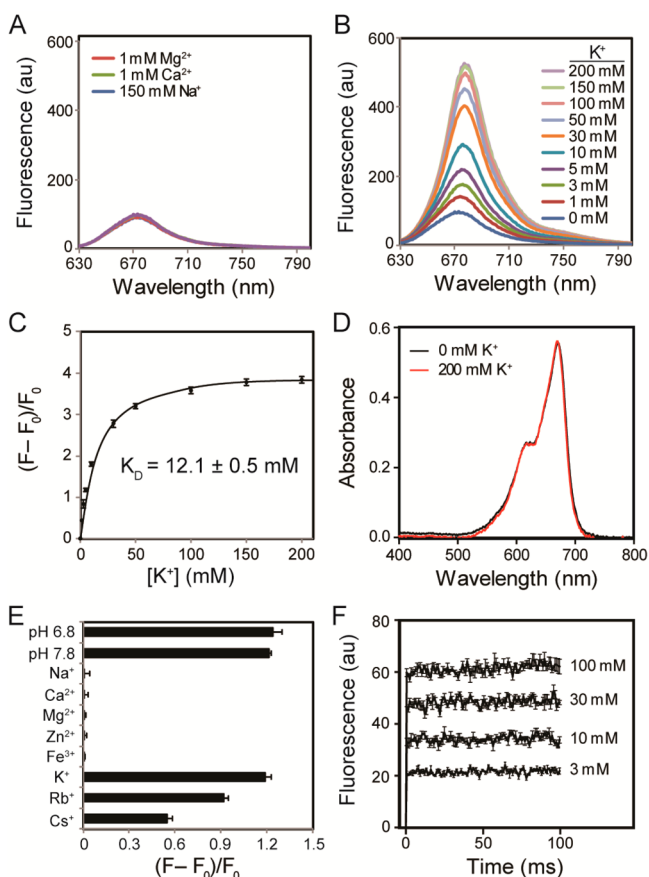


**Figure 2.** Fluorescence emission (Ex: 620 nm) and absorbance of K<sub>NIR-1</sub> in 10 mM HEPES. (A) Fluorescence emission in the presence of Mg<sup>2+</sup>, Ca<sup>2+</sup> and Na<sup>+</sup>. (B) Fluorescence emission at various K<sup>+</sup> concentrations in the presence of Mg<sup>2+</sup> (1 mM), Ca<sup>2+</sup> (1.5 mM) and Na<sup>+</sup> (150 mM). (C) Integrated fluorescence intensities at different K<sup>+</sup> concentrations. *F* is the integrated emission intensity between 630 and 800 nm; *F*<sub>0</sub> is the integrated baseline fluorescence intensity (with 0 mM K<sup>+</sup>). (D) Absorbance spectra at 0 and 200 mM K<sup>+</sup>. (E) Fluorescence intensity (*F* - *F*<sub>0</sub>)/*F*<sub>0</sub> as determined in panel C in the presence of various cations [Na<sup>+</sup> (150 mM), Ca<sup>2+</sup> (1.5 mM), Mg<sup>2+</sup> (1 mM), Zn<sup>2+</sup> (0.3 mM), Fe<sup>3+</sup> (50 μM), K<sup>+</sup> (5 mM), Rb<sup>+</sup> (5 mM), and Cs<sup>+</sup> (5 mM)] and at different pH values with 5 mM K<sup>+</sup> present. Unless indicated, the pH was 7.4. (F) Stopped-flow experiments at various K<sup>+</sup> concentrations; emission was collected at all wavelengths above 645 nm. Data were averaged from three experiments; error bars are ±SEM. Data could not be fitted because the equilibrium rate was faster than the mixing time (1.4 ms).

that K<sub>NIR-1</sub> is essentially nonresponsive to physiological concentrations of extracellular Na<sup>+</sup> (150 mM), Ca<sup>2+</sup> (1.5 mM), and Mg<sup>2+</sup> (1 mM). In contrast, the fluorescence emission of K<sub>NIR-1</sub> was highly dependent on K<sup>+</sup> concentration in the presence of these ions (Figure 2B) with an apparent *K*<sub>d</sub> of 12.1 ± 0.5 mM (Figure 2C). The dissociation constant of K<sub>NIR-1</sub> is approximately fivefold lower than previous TAC-based K<sup>+</sup> sensors where the fluorophore was directly conjugated to the K<sup>+</sup> binding domain.<sup>31</sup> The peak emission wavelength of K<sub>NIR-1</sub> is 680 nm (Figure 2B), whereas the peak absorbance was 670

nm with a molar extinction coefficient  $\epsilon_{670} = 39\,800 \pm 100 \text{ L} \cdot \text{mol}^{-1} \cdot \text{cm}^{-1}$  (Figure 2D), enabling excitation with either visible or near-IR light. K<sup>+</sup> binding (200 mM) to K<sub>NIR-1</sub> had no discernible effect on absorbance (Figure 2D). Using oxazine-170 as fluorescent reference standard,<sup>32,33</sup> the quantum yield for apo K<sub>NIR-1</sub>: 0.0597 ± 0.0003 and K<sup>+</sup> bound (200 mM):  $\Phi = 0.289 \pm 0.005$  were determined from three experiments ± SEM (Supporting Information). Much like K<sup>+</sup> channels that bind to and permeate Rb<sup>+</sup> and Cs<sup>+</sup>,<sup>33</sup> K<sub>NIR-1</sub> also responds to these larger but nonphysiological cations (Figure 2E). As expected, smaller diameter transition metals (Zn<sup>2+</sup> and Fe<sup>3+</sup>) had no effect on K<sub>NIR-1</sub> fluorescence. The fluorescence emission of K<sub>NIR-1</sub> is stable at extracellular and intracellular physiological pH 6.8–7.8 (Figure 2E) but begins to increase at pH 6.5 (Figure S1) as protonation starts to compete with K<sup>+</sup> binding. Thus, under suitably buffered conditions, the fluorescence of K<sub>NIR-1</sub> should faithfully report on K<sup>+</sup> accumulation and depletion during physiological and pathophysiological activity.

We next used stopped-flow experiments to determine the K<sup>+</sup> binding kinetics to TAC-oxazine K<sub>NIR-1</sub>. Figure 2F shows the fluorescence responses from rapid mixing (1.4 ms dead time) of K<sub>NIR-1</sub> with different millimolar solutions of K<sup>+</sup>. Even with rapid mixing, the binding between K<sup>+</sup> and K<sub>NIR-1</sub> at all K<sup>+</sup> concentrations reached equilibrium within the dead time of the stopped-flow instrument. The magnitude of the K<sup>+</sup>-dependent fluorescent response confirmed the *K*<sub>d</sub> of K<sub>NIR-1</sub> (Figure 2C) and that the equilibrium between K<sup>+</sup> and K<sub>NIR-1</sub> was reached within ~1 ms, which is faster than previously reported for TAC-based K<sup>+</sup> sensors using fluorescence correlation spectroscopy.<sup>31</sup> Thus, the submillisecond K<sup>+</sup> association and disassociation kinetics of K<sub>NIR-1</sub> are sufficient to rapidly report on changes in K<sup>+</sup> concentration due to ion channel activity at the plasma membrane.

Although the dissociation constant of K<sub>NIR-1</sub> is somewhat better suited for extracellular K<sup>+</sup> detection, we determined whether the highly membrane permeant K<sub>NIR-1</sub> could detect intracellular K<sup>+</sup> depletion upon K<sup>+</sup> channel opening (Figure 3). Chinese hamster ovary (CHO) cells transiently transfected with empty vector (pCDNA3.1) or a voltage-gated K<sup>+</sup> channel (Shaker-IR) were treated with 50 μM K<sub>NIR-1</sub> for 3 min, and the excess reagent was removed before forming a gigaseal with a single cell (Figure 3A, dotted circles). Whole cell patch clamp fluorometry (Figure 3B) with untransfected cells (–) showed no voltage-dependent currents (*I*) or change in fluorescence ( $\Delta F/F_0$ ). In contrast, Shaker-IR expressing cells showed robust outward currents with depolarizing voltages ≥0 mV (Figure 3C). Simultaneous fluorescent imaging (635 nm excitation) of the whole cell at 10 Hz revealed a concomitant loss in fluorescence that was commensurate with the outward K<sup>+</sup> currents during the 2 s depolarization. The kinetics of the fluorescence signals were substantially slower than the currents, which was consistent with cytoplasmic K<sup>+</sup> depletion at the Shaker-IR intracellular vestibule. Upon channel closing by repolarization to –80 mV, the current rapidly returned to zero (<100 ms), whereas it required seconds for the fluorescent signal to return to the prepolarization values. On the basis of the submillisecond association and disassociation kinetics between K<sup>+</sup> and K<sub>NIR-1</sub> in stopped-flow experiments (Figure 2F), the  $\Delta F/F_0$  kinetics in Figure 3C are consistent with intracellular K<sup>+</sup> depletion during channel opening followed by reestablishment of the cytoplasmic K<sup>+</sup> concentration after channel closing. The extremely long time to restore cellular K<sup>+</sup>

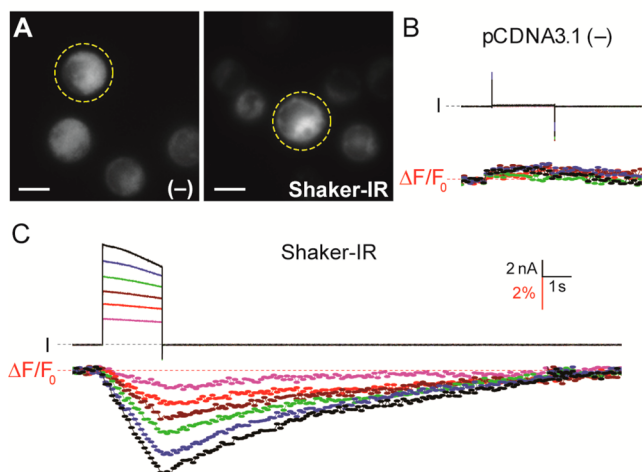


**Figure 3.** Fluorescent detection of  $K^+$  depletion in cells. (A) Wide field images of CHO cells transiently transfected with empty pCDNA3.1 plasmid (–) or Shaker-IR DNA and labeled with  $50 \mu\text{M}$   $K_{\text{NIR}}-1$ . Yellow dotted circles indicate the patch clamped cell in the field of view; fluorescent image scale bars represents  $10 \mu\text{m}$ . Voltage-clamp fluorometry traces for (B) pCDNA3.1 (–) and (C) Shaker-IR: cells were held at  $-80 \text{ mV}$ , and currents ( $I$ ) were elicited from  $2 \text{ s}$  command voltages from  $0$  to  $100 \text{ mV}$  in  $20 \text{ mV}$  increments. Total cellular fluorescence was simultaneously collected at  $10 \text{ Hz}$  by  $10 \text{ ms}$  excitation at  $635 \text{ nm}$ ;  $F_0$  is the average fluorescence intensity of the first ten data points before the test depolarization. Voltage clamp fluorometry scale bars are for both panels B and C; dotted line indicates zero current or change in fluorescence.

to steady state concentrations highlights the importance of the  $\text{Na}^+/\text{K}^+$ -ATPase in maintaining the cellular  $K^+$  and  $\text{Na}^+$  gradients in electrically excitable cells.

Our synthesis of TAC-oxazine  $K_{\text{NIR}}-1$  has several advantages over previous syntheses of visible-light  $K^+$  sensors. First, selective halogenation of the PET donor greatly expands the repertoire of chemistries to attach a fluorophore to the TAC ion binding domain. For example, the Sonogashira coupling described herein should enable the synthesis of a wide palette of fluorescent  $K^+$  sensors using alkynyl-derivatized fluorophores that have become commercially available due to the emergence of bioorthogonal Huisgen 1,3-dipolar cycloadditions (click chemistry). Second, the absorption and emission spectra of TAC-oxazine  $K_{\text{NIR}}-1$  enable  $K^+$  detection using near-IR light, which has better tissue penetration and reduced autofluorescence compared to that of visible light.<sup>26</sup> In addition, TAC-oxazine  $K_{\text{NIR}}-1$  can be utilized with the standard repertoire of visible-light calcium sensors<sup>18–20</sup> and channel rhodopsins,<sup>34,35</sup> negating the need for electrodes and enabling the visualization of multiple ion activities over the landscape of a cell, neuronal circuit, or brain slice. Lastly, the modular synthesis of the oxazine dye will enable the synthesis of chemically reactive derivatives of  $K_{\text{NIR}}-1$  that can be conjugated to membrane proteins<sup>36</sup> and/or the cell surface<sup>37</sup> to detect extracellular  $K^+$  accumulation and depletion.

## EXPERIMENTAL SECTION

**General Experimental Procedures.** Materials were obtained from commercial suppliers and used without further purification. The final oxazine compound was purified by RP HPLC. NMR spectra were recorded in  $\text{CDCl}_3$ ,  $\text{CD}_3\text{OD}$ , or  $\text{DMSO}-d_6$  on a  $400 \text{ MHz}$

spectrometer. HRMS were obtained on a Q-TOF mass spectrometer equipped with an ESI source.

**UV–Visible and Fluorescence Experiments.** Unless otherwise stated, all UV–visible and fluorescence experiments were performed at  $14 \mu\text{M}$   $K_{\text{NIR}}-1$  in  $10 \text{ mM}$  HEPES solutions ( $\text{pH}$  7.4) using acetonitrile as a vehicle ( $0.5\%$  final concentration) in  $3 \text{ mL}$  quartz cuvettes ( $1 \text{ cm}$  optical path length). Excitation wavelength ( $\lambda_{\text{ex}}$ ) was  $620 \text{ nm}$ , and slit width was  $3 \text{ nm}$ . All measurements were corrected for dilution when aliquots of the different test cation solutions significantly changed the total volume. Stock solutions of  $\text{MgCl}_2$  ( $0.30 \text{ M}$ ),  $\text{CaCl}_2$  ( $0.30 \text{ M}$ ),  $\text{NaCl}$  ( $5.4 \text{ M}$ ),  $\text{KCl}$  ( $4.0 \text{ M}$ ),  $\text{ZnCl}_2$  ( $30 \text{ mM}$ ),  $\text{FeCl}_3$  ( $0.5 \text{ mM}$ ),  $\text{RbCl}$  ( $0.5 \text{ M}$ ), and  $\text{CsCl}$  ( $0.5 \text{ M}$ ) were used.

**Stopped-Flow Fluorescence Measurements.** A Hi-Tech Scientific SF-61DX2 stopped-flow system was used to estimate the time course of  $K^+$  binding to  $K_{\text{NIR}}-1$ .  $K_{\text{NIR}}-1$  ( $150 \mu\text{L}$  of a  $14 \mu\text{M}$  solution in  $10 \text{ mM}$  HEPES  $\text{pH}$  7.4) was mixed with various concentrations ( $6$ – $200 \text{ mM}$ ) of  $K^+$  in  $10 \text{ mM}$  HEPES  $\text{pH}$  7.4 and injected into the light path of the flow cell within  $1.4 \text{ ms}$  using a pneumatic drive system. Excitation was at  $620 \text{ nm}$  ( $5 \text{ nm}$  slit width); emission of all wavelengths above  $645 \text{ nm}$  was collected with a photomultiplier. The flow cell and solution reservoirs were at room temperature. Only steady state fluorescence was observed, indicating the equilibrium binding between  $K_{\text{NIR}}-1$  and  $K^+$  occurs within  $1 \text{ ms}$ .

**Whole Cell Patch Clamp Fluorometry.** CHO cell maintenance and transient transfection protocol are listed in the Supporting Information. Transfected CHO cells were trypsinized and seeded on a glass bottom culture dish for  $2 \text{ h}$  and then labeled with  $K_{\text{NIR}}-1$  ( $50 \mu\text{M}$ ) in PBS ( $0.5\%$  final acetonitrile concentration) at RT for  $3 \text{ min}$ ; transfected cells were identified using an inverted light microscope (Axiovert 40 CFL; Carl Zeiss, Inc.), and the currents were recorded in the whole cell patch configuration at room temperature ( $24 \pm 2 \text{ }^\circ\text{C}$ ) using glass pipettes (electrode resistance:  $2.0$ – $3.0 \text{ M}\Omega$ ) filled with internal solution (in  $\text{mM}$ ):  $126 \text{ KCl}$ ,  $2 \text{ MgSO}_4$ ,  $0.5 \text{ CaCl}_2$ ,  $5 \text{ EGTA}$ ,  $4 \text{ K}_2\text{-ATP}$ ,  $0.4 \text{ GTP}$ , and  $25 \text{ HEPES}$  at  $\text{pH}$  7.2 adjusted with  $\text{KOH}$ . Bath solution contained (in  $\text{mM}$ ):  $145 \text{ NaCl}$ ,  $4 \text{ KCl}$ ,  $2 \text{ CaCl}_2$ ,  $1 \text{ MgCl}_2$ ,  $10 \text{ glucose}$ , and  $10 \text{ HEPES}$  at  $\text{pH}$  7.4 adjusted with  $\text{NaOH}$ . Cells were imaged at  $10 \text{ Hz}$  using a CoolLED pE-4000 light source (exposure time =  $10 \text{ ms}$ ),  $63 \times 1.4 \text{ N.A.}$  oil immersion objective, a Chroma Quad filter set ( $89402:391-32/479-33/554-24/638-31$ ), and a Zyla sCMOS camera (ANDOR). GFP and KNIR were excited ( $10 \text{ ms}$ ) at  $460 \text{ nm}$  channel (light power =  $30\%$ ) and  $635 \text{ nm}$  channel (light power =  $10\%$ ), respectively. The patch clamp (Axopatch 200B), light source, and camera were controlled with Clampex 10.5 (Molecular Devices); fluorescent images were collected ( $10 \text{ Hz}$ ,  $4 \times 4$  binning) and processed using open source software (micromanager and ImageJ).  $F_0$  is the average fluorescence intensity of the first ten data points before the test depolarization.

**Synthetic Methods and Compound Characterization.** *TAC-Br* (2). Bromination of triazacryptand **1** was carried out according to a previously reported aryl bromination procedure.<sup>38</sup> Triazacryptand **1**<sup>23</sup> ( $220 \text{ mg}$ ,  $0.32 \text{ mmol}$ ,  $1.0$  equiv) was dissolved in  $\text{CH}_2\text{Cl}_2$  ( $5 \text{ mL}$ ) and cooled to  $0 \text{ }^\circ\text{C}$  in an ice bath. A  $0.55 \text{ M}$  stock solution of bromine in dry  $\text{CH}_2\text{Cl}_2$  was added dropwise by syringe ( $0.63 \text{ mL}$ ,  $0.35 \text{ mmol}$ ,  $1.1$  equiv) to the above solution over a  $5 \text{ min}$  period. After  $10 \text{ min}$  of stirring, the ice bath was removed, and the mixture was stirred at room temperature for an additional  $1.25 \text{ h}$ . The reaction was cooled again to  $0 \text{ }^\circ\text{C}$  in an ice bath, and another aliquot of the  $0.55 \text{ M}$  stock solution of bromine in dry  $\text{CH}_2\text{Cl}_2$  was added via syringe ( $0.63 \text{ mL}$ ,  $0.35 \text{ mmol}$ ,  $1.1$  equiv). After  $10 \text{ min}$  of stirring, the ice bath was removed, and the mixture was stirred at ambient temperature for an additional  $1.25 \text{ h}$ . The reaction was quenched by adding  $10\%$  aqueous  $\text{NaOH}$  ( $10 \text{ mL}$ ) and saturated aqueous  $\text{Na}_2\text{S}_2\text{O}_3$  solution ( $10 \text{ mL}$ ). The organic layer was washed with water ( $10 \text{ mL}$ ), dried with  $\text{Na}_2\text{SO}_4$ , filtered, and concentrated under reduced pressure to give **2** as a brown solid ( $237 \text{ mg}$ ,  $95\%$ ), which was used in the next step without further purification.  $^1\text{H NMR}$  ( $\text{CDCl}_3$ ,  $400 \text{ MHz}$ ):  $\delta$  6.96–7.01 (m, 3H), 6.87 (d,  $J = 7.8$ , 2H), 6.65 (d,  $J = 7.8$ , 2H), 6.56 (s, 2H), 4.12–4.18 (m, 2H), 3.98–4.01 (m, 4H), 3.89–3.92 (m, 4H), 3.78–3.80 (m, 2H), 3.59–3.73 (m, 16H), 3.46 (s, 3H), 3.40–3.45 (m, 4H), 3.26–3.33 (m, 4H), 2.24 (s, 6H).  $^{13}\text{C NMR}$  ( $\text{CDCl}_3$ ,  $100 \text{ MHz}$ ):  $\delta$  153.3, 153.1, 138.3, 137.7,

132.8, 124.6, 123.0, 121.6, 121.2, 117.4, 114.5, 114.1, 71.4, 71.2, 70.2, 68.3, 67.2, 59.3, 54.1, 53.2, 21.3. HRMS (ESI):  $m/z$  calculated for  $C_{39}H_{55}BrN_3O_8$  ( $[M + H]^+$ ): 772.3173; found: 772.3169.

**1-Ethyl-7-methoxy-1,2,3,4-tetrahydroquinoline (11).** Potassium carbonate (1.2 g, 8.4 mmol, 1.5 equiv) was added to a solution of 7-methoxy-1,2,3,4-tetrahydroquinoline (**5**)<sup>30</sup> (0.91 g, 5.6 mmol, 1.0 equiv) in *N,N*-dimethylformamide (DMF) (5 mL). Ethyl iodide (0.54 mL, 6.8 mmol, 1.2 equiv) was added, and the reaction was stirred at 65 °C for 18 h. The mixture was allowed to cool to room temperature, diluted with water (80 mL), and acidified to pH 3 with 1 M HCl. The aqueous phase was extracted with ethyl acetate (1 × 80 mL, 5 × 50 mL), and the combined organic phases were washed with water (3 × 60 mL) and brine (80 mL) and dried over  $Na_2SO_4$ . The solvent was evaporated under vacuum, and the crude product was purified by flash column chromatography on silica (100% hexanes to acetone:hexanes 5:95) to yield **11** as a yellow oil (0.91 g, 85%).  $R_f$  = 0.58 (silica/ethyl acetate:hexanes 1:19). <sup>1</sup>H NMR ( $CDCl_3$ ):  $\delta$  6.84 (d, 1H,  $J$  = 8.1 Hz), 6.18 (d, 1H,  $J$  = 2.1 Hz), 6.13 (dd, 1H,  $J$  = 2.4 Hz, 8.1 Hz), 3.78 (s, 3H), 3.32 (q, 2H,  $J$  = 7.1 Hz), 3.24 (t, 2H,  $J$  = 5.6 Hz), 2.68 (t, 2H,  $J$  = 6.4 Hz), 1.96–1.9 (m, 2H), 1.14 (t, 3H,  $J$  = 7.1 Hz). <sup>13</sup>C NMR ( $CDCl_3$ ):  $\delta$  159.6, 146.1, 129.7, 115.6, 99.8, 97.6, 55.4, 48.6, 45.7, 27.8, 22.8, 11.1. HRMS (ESI)  $m/z$  calculated for  $C_{12}H_{18}NO_2$ : 192.1388 ( $[M + H]^+$ ); found: 192.1379.

**(1-Ethyl-7-methoxy-1,2,3,4-tetrahydroquinolin-6-yl)-(4-nitrophenyl)diazene (3).** 4-Nitrobenzenediazonium tetrafluoroborate (0.57 g, 2.4 mmol, 1.0 equiv) was suspended in 10% aqueous  $H_2SO_4$  (1.6 mL) and added dropwise to a solution of **11** (0.46 g, 2.4 mmol, 1.0 equiv) in methanol (2 mL). The resulting dark purple solution was stirred at room temperature for 1 h and cooled in an ice bath. The reaction was neutralized with aqueous  $NH_4OH$  (28–30%), and the resulting precipitate was isolated by filtration and washed with water (300 mL) to give a dark red solid. The crude product was recrystallized from 1-butanol/water to yield **3** as dark purple crystalline solid (0.52 g, 64%).  $R_f$  = 0.14 (silica/ethyl acetate:hexanes 1:19). <sup>1</sup>H NMR ( $CDCl_3$ ):  $\delta$  8.26 (d, 2H,  $J$  = 8.9 Hz), 7.84 (d, 2H,  $J$  = 8.9 Hz), 7.58 (s, 1H), 6.11 (s, 1H), 4.00 (s, 3H), 3.46 (q, 2H,  $J$  = 7.1 Hz), 3.38 (t, 2H,  $J$  = 5.6 Hz), 2.71 (t, 2H,  $J$  = 6.0 Hz), 1.95 (p, 2H,  $J$  = 5.6 Hz, 6.1 Hz), 1.26 (t, 3H,  $J$  = 7.1 Hz). <sup>13</sup>C NMR ( $CDCl_3$ ):  $\delta$  160.3, 158, 151.4, 146.7, 133.6, 124.9, 122.5, 117.7, 116.5, 92.8, 56.5, 49.2, 46.3, 27.5, 22.2, 11.5. HRMS (ESI)  $m/z$  calculated for  $C_{18}H_{21}N_4O_3$ : 341.1614 ( $[M + H]^+$ ); found: 341.1625.

**1-(Prop-2-yn-1-yl)-1,2,3,4-tetrahydroquinolin-7-ol (12).** 7-Hydroxy-1,2,3,4-tetrahydroquinoline (**6**)<sup>30</sup> (0.60 g, 4.0 mmol, 1.0 equiv) and  $K_2CO_3$  (0.66 g, 4.8 mmol, 1.2 equiv) were combined in DMF (5 mL). 3-Bromo-1-propyne (0.9 mL of an 80 wt % solution in toluene, 6.0 mmol, 1.5 equiv) was added, and the reaction was stirred at 60 °C for 1.5 h. The reaction was cooled and partitioned between ethyl acetate (100 mL) and water (20 mL). The aqueous layer was washed with ethyl acetate (3 × 20 mL), and the organic layers were combined, dried over  $Na_2SO_4$ , filtered, and concentrated under vacuum. The crude product was purified by flash chromatography on silica (ethyl acetate:hexanes 1:4) to yield **12** as a brown oil, which acquired a light pink color upon standing (0.52 g, 69%).  $R_f$  = 0.35 (silica/ethyl acetate:hexanes 1:4). <sup>1</sup>H NMR ( $CDCl_3$ , 400 MHz):  $\delta$  6.82 (d,  $J$  = 8.0 Hz, 1H), 6.24 (d,  $J$  = 3.6 Hz), 6.16 (dd,  $J$  = 8.0 Hz,  $J$  = 3.6 Hz, 1H), 4.68 (s, 1H), 3.97 (d,  $J$  = 2.4 Hz, 2H), 3.27 (t,  $J$  = 5.6 Hz, 2H), 2.69 (t,  $J$  = 6.4 Hz, 2H), 2.17 (t,  $J$  = 2.4 Hz, 1H), 2.01–1.94 (m, 2H). <sup>13</sup>C NMR ( $CDCl_3$ , 100 MHz):  $\delta$  154.7, 145.5, 129.8, 116.4, 104.2, 99.3, 79.5, 71.8, 49.1, 40.8, 26.9, 22.5. HRMS (ESI)  $m/z$  calculated for  $C_{12}H_{14}NO$  ( $[M + H]^+$ ): 188.1070; found 188.1065.

**1-(Prop-2-yn-1-yl)-1,2,3,4-tetrahydroquinolin-7-yl acetate (4).** The product **12** (200 mg, 1.1 mmol, 1.0 equiv), acetic anhydride (402  $\mu$ L, 4.4 mmol, 4.0 equiv), and triethylamine (306  $\mu$ L, 2.2 mmol, 2.0 equiv) were dissolved in  $CH_2Cl_2$  (5 mL), and the reaction was stirred at room temperature for 18 h. The reaction was washed with saturated aqueous  $Na_2CO_3$  (20 mL) and 0.5 M HCl (20 mL), dried over  $MgSO_4$ , and filtered, and the solvent was removed. Purification by flash chromatography on silica (ethyl acetate:hexanes 5:95) yielded **4** as a yellow oil, which became a white solid upon standing (192 mg, 71%).  $R_f$  = 0.33 (silica/ethyl acetate:hexanes 1:19). <sup>1</sup>H NMR ( $CDCl_3$ ,

400 MHz):  $\delta$  6.97 (d,  $J$  = 8.0 Hz, 1H), 6.42 (d,  $J$  = 2.0 Hz, 1H), 6.40 (dd,  $J$  = 8.0 Hz,  $J$  = 2.0 Hz), 3.97 (d,  $J$  = 2.4 Hz, 2H), 3.29 (t,  $J$  = 5.6 Hz, 2H), 2.74 (t,  $J$  = 6.4 Hz, 2H), 2.29 (s, 3H), 2.20 (t,  $J$  = 2.4 Hz, 1H), 2.02–1.96 (m, 2H). <sup>13</sup>C NMR ( $CDCl_3$ , 100 MHz):  $\delta$  169.9, 149.9, 145.4, 129.5, 121.4, 110.0, 105.1, 79.3, 72.0, 48.9, 40.7, 27.2, 22.2, 21.2. HRMS (ESI):  $m/z$  calculated for  $C_{14}H_{16}NO_2$  ( $[M + H]^+$ ): 230.1181; found: 230.1171.

**11-Ethyl-1-(prop-2-yn-1-yl)-2,3,4,8,9,10-hexahydro-1H-dipyrido[3,2-b:2',3'-i]phenoxazin-11-ium chloride (7).** The product **3** (20 mg, 0.59 mmol, 1.0 equiv) and the product **4** (13 mg, 0.59 mmol, 1.0 equiv) were combined in 0.5 mL of 1.5% HCl (37% HCl:ethanol:water 0.5:10:1 mL) and stirred at 80 °C for 4 h. The resulting dark green reaction was concentrated under vacuum. Purification by column chromatography on silica (methanol: $CH_2Cl_2$  1:10) yielded the chloride salt of **7** as a dark blue solid (13 mg, 59%).  $R_f$  = 0.59 (silica:MeOH/ $CH_2Cl_2$  1:9). <sup>1</sup>H NMR ( $CDCl_3$ , 400 MHz):  $\delta$  7.47 (s, 1H), 7.36 (s, 1H), 7.29 (s, 1H), 6.51 (s, 1H), 3.72–3.68 (m, 2H), 3.55 (t,  $J$  = 6.8 Hz, 4H), 3.49 (s, 2H), 2.87 (t,  $J$  = 6.0 Hz, 4H), 2.17 (s, 1H), 2.08–1.97 (m, 4H), 1.34 (t,  $J$  = 7.2 Hz, 3H). <sup>13</sup>C NMR ( $CDCl_3$ , 100 MHz):  $\delta$  155.1, 153.4, 146.3, 132.8, 130.7, 130.4, 130.3, 130.2, 128.5, 95.6, 94.9, 76.5, 73.7, 60.9, 57.8, 50.1, 26.9, 26.8, 20.7, 20.4, 10.4. HRMS (ESI)  $m/z$  calculated for  $C_{23}H_{24}N_3O$  ( $M^+$ ): 358.1914; found: 358.1917.

**(E)-1-(3-(4,4,5,5-Tetramethyl-1,3,2-dioxaborolan-2-yl)allyl)-1,2,3,4-tetrahydroquinolin-7-yl acetate (9).** The product **4** (220 mg, 0.74 mmol, 1.0 equiv), pinacolborane (110 mg, 0.89 mmol, 1.2 equiv), and triethylamine (8.6  $\mu$ L, 0.060 mmol, 0.086 equiv) were combined in a sealable reaction vessel, and the vessel was purged with Ar for 10 min.  $ZrCp_2HCl$  (8.1 mg, 0.031 mmol, 0.042 equiv) was quickly added; the vessel was sealed, and the reaction was stirred at 60 °C for 15 h under Ar. Reaction contents were dissolved in ethyl acetate:hexanes (1:9), and the product was purified by flash chromatography on silica (ethyl acetate:hexanes 1:99 to 3:97) to yield **9** as a yellow oil (127 mg, 48%).  $R_f$  = 0.15 (silica/ethyl acetate:hexanes 1:19). <sup>1</sup>H NMR ( $CD_3OD$ , 400 MHz):  $\delta$  6.79 (dd,  $J$  = 12 Hz,  $J$  = 8 Hz, 1H), 6.09–6.01 (m, 2H), 5.62 (d,  $J$  = 18 Hz, 1H), 4.86 (m, 2H), 3.20–3.18 (m, 2H), 2.64–2.61 (m, 2H), 2.06 (s, 3H), 1.94–1.86 (m, 2H), 1.24 (d, 12H). <sup>13</sup>C NMR ( $CD_3OD$ , 100 MHz):  $\delta$  167.9, 155, 145.7, 136.2, 129.5, 124.7, 113.1, 104.3, 100.9, 82.4, 74.5, 71.8, 50.9, 41.4, 23.4, 23.5, 22.3, 17.0. HRMS (ESI):  $m/z$  calculated for  $C_{20}H_{29}BNO_4$  ( $[M + H]^+$ ): 358.2190; found: 358.2186.

**(E)-11-Ethyl-1-(3-(4,4,5,5-tetramethyl-1,3,2-dioxaborolan-2-yl)allyl)-2,3,4,8,9,10-hexahydro-1H-dipyrido[3,2-b:2',3'-i]phenoxazin-11-ium chloride salt (8).** The product **3** (28 mg, 0.095 mmol, 1.0 equiv) and the borane ester **9** (40 mg, 0.095 mmol, 1.0 equiv) were combined in 0.5 mL of 1.5% HCl (37% HCl:ethanol:water 0.5:10:1 mL) and stirred at 80 °C for 4 h. The resulting dark green reaction was concentrated under vacuum. Purification by column chromatography on silica (methanol: $CH_2Cl_2$  1:10) yielded **8** as a dark blue solid (14 mg, 29%).  $R_f$  = 0.57 (silica/MeOH: $CH_2Cl_2$  3:17). <sup>1</sup>H NMR ( $CDCl_3$ , 400 MHz):  $\delta$  6.96 (s, 1H), 6.94 (s, 1H), 6.41–6.37 (m, 4H), 3.97 (d,  $J$  = 2.7 Hz, 2H), 3.29 (m, 4H), 2.72 (t,  $J$  = 6.8 Hz, 4H), 2.28 (s, 12H). 2.17 (m, 3H), 2.00–1.97 (m, 4H). <sup>13</sup>C NMR ( $CDCl_3$ , 100 MHz):  $\delta$  155.2, 153.5, 148.0, 130.8, 130.3, 128.7, 121.3, 111.1, 74.8, 73.8, 61.1, 57.9, 50.2, 27.1, 26.9, 20.8, 20.6, 10.5. HRMS (ESI):  $m/z$  calculated for  $C_{29}H_{37}BN_3O_3$  ( $M^+$ ): 484.9222; found: 484.9227.

**TAC-N-propargyl-1,2,3,4-tetrahydroquinolin-7-ol (10).** A reaction vessel containing TAC-Br **2** (271 mg, 0.35 mmol, 1.0 equiv) and product **4** (250 mg, 1.1 mmol, 3.1 equiv) was purged with Ar for 10 min, and the Ar was removed by applying high vacuum. The above procedure was repeated two more times. DMF (1.0 mL) and pyrrolidine (1.0 mL) were injected into the reaction vessel, and Ar was bubbled through the resulting solution for 10 min.  $Pd(PPh_3)_4$  (66 mg, 0.058 mmol, 0.17 equiv) and CuI (9.5 mg, 0.050 mmol, 0.014 equiv) were quickly added, and the reaction was purged with Ar for 5 min and stirred at 80 °C for 18 h. Solvents were removed under high vacuum, and the resulting brown residue was purified by flash chromatography on neutral alumina ( $CH_2Cl_2$  to methanol: $CH_2Cl_2$  1:9). The purified product was dissolved in 1:2 methanol/ $CH_2Cl_2$  (6 mL); SiliaMet DMT (450 mg of silica with 0.60 mmol/g scavenger loading, 5 equiv)

was added, and the reaction was refluxed at 80 °C for 4 h. The silica was filtered off, and the solvent was removed to yield **10** as a brown oil (108 mg, 35%). A 30 mg aliquot of **10** was purified by preparative HPLC according to the conditions below to obtain a sample with sufficient purity for spectroscopic characterization. Method started at 30% solvent B (0.1% trifluoroacetic acid in acetonitrile) and 70% solvent A (0.1% trifluoroacetic acid in water), then 30–60% solvent B over 15 min, then 60–100% solvent B over 1 min, and then 100% solvent B for 5 min. HPLC absorbance detector was set at 254 nm. The product eluted at 15.0 min. HPLC fractions were combined and lyophilized to yield **10** as a brown oil.  $R_f = 0.30$  (neutral alumina/methanol:CH<sub>2</sub>Cl<sub>2</sub> 1:49). <sup>1</sup>H NMR (CDCl<sub>3</sub>, 400 MHz):  $\delta$  7.08 (d,  $J = 8.0$  Hz, 1H), 6.96–6.82 (m, 6H), 6.75 (m, 2H), 6.20 (dd,  $J = 6.0$  Hz,  $J = 2.4$  Hz, 1H), 6.03 (d,  $J = 2.4$  Hz, 1H), 4.21 (t,  $J = 4.2$  Hz, 4H), 4.10 (t,  $J = 4.4$  Hz, 2H), 3.79–3.61 (m, 27H), 3.40 (t,  $J = 4.8$  Hz, 1H), 3.35 (s, 3H), 3.29–3.26 (m, 8H), 2.69 (t,  $J = 6.4$  Hz, 4H), 2.36 (s, 6H), 1.94–1.88 (m, 2H). <sup>13</sup>C NMR (CDCl<sub>3</sub>, 100 MHz):  $\delta$  153.3, 150.4, 148.8, 131.8, 129.5, 127.4, 121.6, 118.6, 112.0, 109.5, 102.3, 98.5, 81.9, 68.2, 68.1, 67.6, 65.3, 64.2, 51.0, 50.5, 49.9, 39.2, 28.5, 23.7, 19.9, 18.5, 18.2. HRMS (ESI):  $m/z$  calculated for C<sub>51</sub>H<sub>66</sub>N<sub>4</sub>O<sub>9</sub>Na ([M + Na]<sup>+</sup>): 901.4727; found: 901.4726.

**TAC-N-propan-1,2,3,4-tetrahydroquinolin-7-ol (13)**. The TAC-alkyne **10** (104 mg, 0.12 mmol, 1.0 equiv) and tosyl hydrazide (440 mg, 2.4 mmol, 20 equiv) were dissolved in 1,2-dimethoxyethane (1.0 mL) and stirred at 80 °C. A solution of sodium acetate (190 mg, 2.4 mmol, 20 equiv) in water (1.0 mL) was added dropwise to the above solution over a period of 6 h. The resulting mixture was stirred at 80 °C for 18 h and then stirred at room temperature for another 4 h. The reaction was partitioned between ethyl acetate (10 mL) and water (5 mL), and the aqueous phase was extracted with ethyl acetate (3 × 10 mL). The organic layers were combined, dried over MgSO<sub>4</sub>, filtered and solvent was removed. Purification by flash chromatography on neutral alumina (CH<sub>2</sub>Cl<sub>2</sub> to methanol/CH<sub>2</sub>Cl<sub>2</sub> 1:9) yielded **13** as a brown oil (76 mg, 72%). A 30 mg aliquot of **13** was purified by preparative HPLC according to the conditions below to obtain a sample with sufficient purity for spectroscopic characterization. Method started at 30% solvent B (0.1% trifluoroacetic acid in acetonitrile) and 70% solvent A (0.1% trifluoroacetic acid in water), then 30–60% solvent B over 15 min, then 60–100% solvent B over 1 min, then 100% solvent B for 5 min. HPLC absorbance detector was set at 254 nm. The product eluted at 15.7 min. HPLC fractions were combined and lyophilized to yield **13** as a brown oil.  $R_f = 0.32$  (neutral alumina/methanol:CH<sub>2</sub>Cl<sub>2</sub> 1:49). <sup>1</sup>H NMR (CDCl<sub>3</sub>, 400 MHz):  $\delta$  7.12 (dd,  $J = \text{Hz}$ ,  $J = \text{Hz}$ , 1H), (m, 7H), 6.74 (m, 2H), 6.20 (dd,  $J = 2.8$  Hz,  $J = 8.4$  Hz, 1H), 6.03 (d,  $J = 2.8$  Hz, 1H), 4.23–4.20 (m, 4H), 4.12–4.09 (m, 2H), 3.79–3.61 (m, 26H), 3.43–3.40 (m, 4H), 3.35 (s, 3H), 3.29–3.26 (m, 8H), 2.69 (t,  $J = 6.4$  Hz, 2H), 2.36 (s, 6H), 1.94–1.84 (m, 4H), 1.49–1.45 (m, 2H). <sup>13</sup>C NMR (CDCl<sub>3</sub>, 100 MHz):  $\delta$  162.7, 152.7, 146.5, 139.5, 134.2, 127.7, 121.3, 115.3, 113.6, 113.2, 71.2, 67.5, 67.0, 55.1, 58.9, 52.4, 50.1, 36.4, 31.3, 21.1. HRMS (ESI):  $m/z$  calculated for C<sub>51</sub>H<sub>70</sub>N<sub>4</sub>O<sub>9</sub>Na ([M + Na]<sup>+</sup>): 905.5040; found: 905.5042.

**K<sub>NIR</sub>-1**. The aryl azobenzene **3** (28 mg, 0.095 mmol, 1.0 equiv) and TAC-alkane **13** (40 mg, 0.095 mmol, 1.0 equiv) were combined in acetic acid (0.5 mL) and stirred at 80 °C for 18 h. The resulting dark green reaction was concentrated under vacuum and purified by preparative HPLC according to the conditions. Method started at 30% solvent B (0.1% trifluoroacetic acid in acetonitrile) and 70% solvent A (0.1% trifluoroacetic acid in water), then 30–60% solvent B over 15 min, then 60–100% solvent B over 1 min, and then 100% solvent B for 5 min. HPLC absorbance detector was set at 254 nm. The product eluted at 15.7 min. HPLC fractions were combined and lyophilized to yield the trifluoroacetate salt of **K<sub>NIR</sub>-1** as a blue solid (mg, 22%), which was first converted to the hydroxide salt and then to the acetate salt by passing through DOWEX 1 × 8 200–400 hydroxide and acetate anion exchange columns.  $R_f = 0.20$  (silica/methanol:CH<sub>2</sub>Cl<sub>2</sub> 1:9). <sup>1</sup>H NMR (CD<sub>3</sub>OD, 400 MHz):  $\delta$  7.58 (d,  $J = 9.6$  Hz, 2H), 7.45 (d,  $J = 14.4$  Hz, 2H), 7.22 (d, 8.0 Hz, 1H), 7.03–6.98 (m, 5H), 6.92 (s, 2H), 6.85 (d,  $J = 8.0$  Hz, 1H), 6.60 (s, 1H), 4.35–4.20 (m, 6H), 4.25–3.85 (m, 12H), 3.85–3.75 (m, 5H), 3.75–3.50 (m, 17H), 3.50–

3.35 (m, 5H), 3.31 (s, 3H), 3.85–3.75 (m, 4H), 2.70 (t,  $J = 7.2$  Hz, 2H), 2.30 (s, 6H), 2.20–1.80 (m, 6H), 1.38 (t,  $J = 7.2$  Hz, 3H). <sup>13</sup>C NMR (DMSO-*d*<sub>6</sub>, 100 MHz):  $\delta$  172.5, 163.5, 156.0, 152.9, 152.8, 151.3, 151.1, 147.4, 131.9, 123.9, 122.2, 121.6, 121.5, 121.4, 116.7, 114.5, 114.4, 96.9, 95.3, 70.7, 70.5, 70.3, 67.9, 58.5, 52.6, 52.5, 52.5, 35.5, 32.5, 27.1, 21.5, 14.5, 11.8. HRMS (ESI):  $m/z$  calculated for C<sub>62</sub>H<sub>81</sub>N<sub>6</sub>O<sub>9</sub>Na ([M + Na]<sup>2+</sup>): 527.3069; found: 527.3068.

## ■ ASSOCIATED CONTENT

### Supporting Information

The Supporting Information is available free of charge on the ACS Publications website at DOI: 10.1021/acs.joc.7b00845.

Experimental procedures, compound characterization, and supplementary figures (PDF)

## ■ AUTHOR INFORMATION

### Corresponding Author

\*E-mail: william.kobertz@umassmed.edu

### ORCID

Stephen C. Miller: 0000-0001-7154-7757

William R. Kobertz: 0000-0003-3628-7974

### Present Address

<sup>§</sup>S.M.P.: Department of Pure and Applied Chemistry, University of Strathclyde, 295 Cathedral Street, Glasgow G1 1XL, United Kingdom.

### Notes

The authors declare no competing financial interest.

## ■ ACKNOWLEDGMENTS

This work was supported by a grant to W.R.K. from the National Institutes of Health (GM-070650). S.C.M. acknowledges support from the NIH (Grant GM-087460), and S.M.P. received fellowship support from the American Heart Association.

## ■ REFERENCES

- Houngaard, J.; Nicholson, C. *J. Physiol.* **1983**, *340*, 359.
- Martin, G.; Morad, M. *J. Physiol.* **1982**, *328*, 205.
- Zifarelli, G.; Pusch, M. *J. Gen. Physiol.* **2010**, *136*, 593.
- Dunn, K. M.; Nelson, M. T. *Circ. J.* **2010**, *74*, 608.
- McCrossan, Z. A.; Abbott, G. W. *Neuropharmacology* **2004**, *47*, 787.
- Nichols, C. G. *Nature* **2006**, *440*, 470.
- Wallinga, W.; Vliek, M.; Wienk, E. D.; Alberink, M. J.; Ypey, D. L. *Proceedings of the 18th Annual International Conference of the IEEE* **1996**, *5*, 1909.
- Shepherd, N.; McDonough, H. B. *Am. J. Physiol.* **1998**, *275*, H852.
- Swift, F.; Stromme, T. A.; Amundsen, B.; Sejersted, O. M.; Sjaastad, I. *J. Appl. Physiol.* **2006**, *101*, 1170.
- Wangemann, P. *Hear. Res.* **2002**, *165*, 1.
- Frohlich, F.; Bazhenov, M.; Iragui-Madoz, V.; Sejnowski, T. J. *Neuroscientist* **2008**, *14*, 422.
- Costa, C.; Tozzi, A.; Rainero, I.; Cupini, L. M.; Calabresi, P.; Ayata, C.; Sarchielli, P. *J. Headache Pain* **2013**, *14*, 62.
- Cannon, S. C. *J. Physiol.* **2010**, *588*, 1887.
- Marban, E. *Nature* **2002**, *415*, 213.
- Ashcroft, F. M. *J. Clin. Invest.* **2005**, *115*, 2047.
- Weiss, J.; Shine, K. I. *Am. J. Physiol.* **1982**, *243*, H318.
- Lee, M. P.; Ravenel, J. D.; Hu, R. J.; Lustig, L. R.; Tomaselli, G.; Berger, R. D.; Brandenburg, S. A.; Litz, T. J.; Bunton, T. E.; Limb, C.; Francis, H.; Gorelikow, M.; Gu, H.; Washington, K.; Argani, P.; Goldenring, J. R.; Coffey, R. J.; Feinberg, A. P. *J. Clin. Invest.* **2000**, *106*, 1447.

- (18) Paredes, R. M.; Etzler, J. C.; Watts, L. T.; Zheng, W.; Lechleiter, J. D. *Methods* **2008**, *46*, 143.
- (19) Chen, T. W.; Wardill, T. J.; Sun, Y.; Pulver, S. R.; Renninger, S. L.; Baohan, A.; Schreiter, E. R.; Kerr, R. A.; Orger, M. B.; Jayaraman, V.; Looger, L. L.; Svoboda, K.; Kim, D. S. *Nature* **2013**, *499*, 295.
- (20) Tian, L.; Hires, S. A.; Mao, T.; Huber, D.; Chiappe, M. E.; Chalasani, S. H.; Petreanu, L.; Akerboom, J.; McKinney, S. A.; Schreiter, E. R.; Bargmann, C. I.; Jayaraman, V.; Svoboda, K.; Looger, L. L. *Nat. Methods* **2009**, *6*, 875.
- (21) Carpenter, R. D.; Verkman, A. S. *Org. Lett.* **2010**, *12*, 1160.
- (22) Zhou, X.; Su, F.; Tian, Y.; Youngbull, C.; Johnson, R. H.; Meldrum, D. R. *J. Am. Chem. Soc.* **2011**, *133*, 18530.
- (23) He, H.; Mortellaro, M. A.; Leiner, M. J.; Fraatz, R. J.; Tusa, J. K. *J. Am. Chem. Soc.* **2003**, *125*, 1468.
- (24) Padmawar, P.; Yao, X.; Bloch, O.; Manley, G. T.; Verkman, A. S. *Nat. Methods* **2005**, *2*, 825.
- (25) Hirata, T.; Terai, T.; Komatsu, T.; Hanaoka, K.; Nagano, T. *Bioorg. Med. Chem. Lett.* **2011**, *21*, 6090.
- (26) Weissleder, R. *Nat. Biotechnol.* **2001**, *19*, 316.
- (27) Eggeling, C.; Widengren, J.; Brand, L.; Schaffer, J.; Felekyan, S.; Seidel, C. A. *J. Phys. Chem. A* **2006**, *110*, 2979.
- (28) Doose, S.; Neuweiler, H.; Sauer, M. *ChemPhysChem* **2009**, *10*, 1389.
- (29) Hintersteiner, M.; Enz, A.; Frey, P.; Jatou, A. L.; Kinzy, W.; Kneuer, R.; Neumann, U.; Rudin, M.; Staufenberg, M.; Stoeckli, M.; Wiederhold, K. H.; Gremlich, H. U. *Nat. Biotechnol.* **2005**, *23*, 577.
- (30) Pauff, S. M.; Miller, S. C. *Org. Lett.* **2011**, *13*, 6196.
- (31) Magzoub, M.; Padmawar, P.; Dix, J. A.; Verkman, A. S. *J. Phys. Chem. B* **2006**, *110*, 21216.
- (32) Rurack, K.; Spieles, M. *Anal. Chem.* **2011**, *83*, 1232.
- (33) Doyle, D. A.; Morais Cabral, J.; Pfuetzner, R. A.; Kuo, A.; Gulbis, J. M.; Cohen, S. L.; Chait, B. T.; MacKinnon, R. *Science* **1998**, *280*, 69.
- (34) Kleinlogel, S.; Feldbauer, K.; Dempski, R. E.; Fotis, H.; Wood, P. G.; Bamann, C.; Bamberg, E. *Nat. Neurosci.* **2011**, *14*, 513.
- (35) Caldwell, J. H.; Herin, G. A.; Nagel, G.; Bamberg, E.; Scheschonka, A.; Betz, H. *J. Biol. Chem.* **2008**, *283*, 24300.
- (36) Hirata, T.; Terai, T.; Yamamura, H.; Shimonishi, M.; Komatsu, T.; Hanaoka, K.; Ueno, T.; Imaizumi, Y.; Nagano, T.; Urano, Y. *Anal. Chem.* **2016**, *88*, 2693.
- (37) Zhang, L.; Bellve, K.; Fogarty, K.; Kobertz, W. R. *Cell Chemical Biology* **2016**, *23*, 1449.
- (38) Metten, B.; Smet, M.; Boens, N.; Dehaen, W. *Synthesis* **2005**, *11*, 1838.